physica pssa status solidi
www.pss-a.com

applications and materials science

Comparative analysis of mechanical properties of Si substrates processed by different routes

Sylvain Gouttebroze[1], Hans Ivar Lange[2], Xiang Ma[1], R. Gløckner[3], Behnaz Emamifard[3], W. Syvertsen[2], Michalis Vardavoulias[4], and Alexander Ulyashin[*,1]

[1] SINTEF MK, Forskningsveien 1, 0314 Oslo, Norway
[2] SINTEF MK, Trondheim, Norway
[3] Elkem Solar, Kristiandsand, Norway
[4] Pyrogenesis, Lavrion, Greece

* Corresponding author: e-mail alexanderg.ulyashin@sintef.no, Phone: +47 93 00 22 24, Fax: +47 22 06 73 50

The purpose of this work is to check the potential of innovative processes for the Si wafers production toward the solar cell industry.[Q1] Studies have been focused on a comparative analysis of mechanical properties of such wafers, since: (i) reduced wafer strength leads to a high breakage rate during subsequent handling and solar cell processing steps, (ii) cracking of solar cells has become one of the major sources of solar module failure and rejection. Therefore while developing new types of wafer materials and processing, it is essential to assess the mechanical strength of the wafers. Mechanical properties of several innovative Si based substrates are estimated. The bending strength measurements of the silicon wafer are performed using the ring-on-ring set-up coupled with a numerical model to obtain estimate of the fracture stress and the Weibull parameters of the fracture distribution. Results are presented for five different materials: sintered Si powder, standard multi-crystalline Si, Czochralski monocrystalline Si, and two types of thermal sprayed Si wafers.

© 2013 WILEY-VCH Verlag GmbH & Co. KGaA, Weinheim

1 Introduction Currently, the PV market is dominated by crystalline silicon solar cells, and about 40% of the silicon module cost is from the silicon wafers. Therefore, a major part of current research activity is concentrated on a search for alternative silicon based solar cell concepts with reduced consumption of high-purity silicon. In conventional Si wafer based solar cell technology, most of the Si material acts as a mechanical carrier for the solar cell structures. However, since most of the optical absorption in Si takes place in the upper 15–30 μm, it is sufficient to use only thin Si layers with thicknesses in this range. Indeed, if special optical confinement schemes are implemented, even thinner layers can be used [1]. In general, thin-film photovoltaics are assumed to become a market dominating technology in the long term and any development in this field is extremely important for the PV industry [2].

To be able to reduce thin Si film solar cell cost, both material and material fabrication costs must be reduced. This can be achieved by growing a high quality "expensive" thin active crystalline Si layer onto a less expensive substrate. Ceramic or glass based materials have been proposed as such substrates. Such option is still envisaged to be cheaper than the use of conventional Si-wafer substrates, as thin film PECVD and PVD deposition processes, for example, have been routinely used to produce high quality thin films for electric and optoelectronic devices at accepted consumer costs. Depending on process conditions, thin Si based-layers of amorphous (a-Si), hydrogenated amorphous (a-Si:H), microcrystalline (μc-Si), or polycrystalline (poly-Si) silicon can be grown on such substrates. For μc-Si-based solar cell structures deposited on glass substrates, energy conversion efficiencies up to 10% have been demonstrated [3]. At the same time solar cells utilizing thin-film polycrystalline Si with an optimum thickness about 20 μm can achieve photovoltaic power conversion efficiencies greater than 19% [4]. However, the use of ceramic and glass substrates for thin Si solar cells have some problems:

Conductivity: Glass and ceramic substrates are non-conductive. Thus, a lot of attention has been directed towards

making a highly conductive back side electrode as well as a system for contacting the electrode after deposition of silicon [5]. Diffusion of aliovalent dopants from the electrode is a big problem. Conducting SiC is being developed as an alternative [6]. However, still a number of problems have to be solved in this approach, since crystallization of Si layers on SiC substrates is rather problematic.

Lattice matching: Glass and ceramic substrates have no crystallographic relation to silicon to aid crystallization at lower temperatures and/or into higher crystallographic quality. Thus, higher temperatures are needed when using, e.g., a higher cost single crystal Si wafer.

Purity: Care must be taken to avoid diffusion of dopants into Si during deposition and post-processing.

Temperature stability: One needs >700–$1000\,^\circ$C for growth of poly-Si. This is marginal for the case of glass substrates. Therefore lower temperatures are used for such processes.

It can be concluded that there is a demand for advanced low-cost substrates, which can be used for thin Si-based solar cell structures. So far such low-cost Si supporting substrates have been based on highly doped Si wafers processed in the same way as conventional Si wafers, i.e., by crystallization of ingots and wafering. Such conventional processing of Si wafers can be substituted by a cost-effective powder-to-wafer processing using ceramics technology, hence avoiding costly crystallization and wafering steps. Such "powder-to-wafer" approach, can simplify the wafer based processing of the supporting Si substrates and therefore relevant thin Si-based solar cells, Usage of a low grade Si feedstock can reduce the cost of Si wafers even further. These low purity substrates can be processed from a low-quality Si powder. When the powder is shaped and sintered into an appropriate substrate, it can be considered as a poly-Si seeding material, which can provide good crystallization conditions for any Si-based layers deposited and annealed at appropriate conditions.

Such substrates have several advantages compared to ceramic or glass substrates: (i) highly doped silicon is conductive. Hence, the substrate can be used as electrode, avoiding any contact problems; (ii) a perfect lattice match will lead to the lowest possible crystallization temperatures for the deposited high purity thin film, (iii) silicon-based low-cost supporting substrates are fully compatible with the deposition/crystallization processes of thin Si layers on top of such substrates.

The concept of crystalline silicon thin-film solar cells on low-purity substrates provides a hope to reduce substantially the consumption of high-purity silicon material and has at the same time potential to reach high efficiencies comparable to wafer silicon solar cells. The goal of this article is to test mechanical properties of Si wafers, processed in frame of an innovative approach based on a thermal spray of Si powder and sintered Si and to compare both Si powder-based substrates with those, which are processed by casting or CZ growth methods.

This article firstly describes the material and samples preparation. Secondly the electrical properties are quickly studied. The measurements and the associated numerical model are presented in the next section. Finally the results are discussed as well as possible explanations for the discrepancies in the material properties and their link to processing routes.

2 Samples material and preparation
2.1 Materials and processing techniques
The original powder (Si feedstock) for the substrates comes from a by-product stream of the Elkem Solar metallurgical process route to produce Elkem Solar Silicon® in a form of Si powder. The quality is in-between the process starting-point: metallurgical grade silicon and the end-point: solar grade silicon. Several types of Si powders in the wide range of particle size distribution (PSD) have been tested. The PSD values were varied in the range of 1–150 μm and were adjusted to the special requirements of each processing techniques used. The following techniques, which utilized as produced Si powder directly without any additional processing or cleaning (like HF dip) steps have been tested: (i) casting of Si ingot from Si powder using a pilot scale vertical gradient freeze (VGF) furnace and (ii) thermal spray of Si powder. Important to underline that in both cases Si powder was covered by native oxide and processing conditions were optimized to reduce this oxide upon the fabrication. In case of a thermal spray technique PSD values were below 100 μm. As-processed Si powder was used for sintering of Spray-1 Si substrates. For the other type of sprayed Si substrates 3% (weight) of Al powder was mixed with the Si powder-based feedstock prior the spraying (Spray 2 substrates).

In case of the casting process, which was carried out using a VGF furnace at SINTEF, Si powders with PSD values up to 150 μm have been used. The silicon powder-based feedstock was melted and solidified. The thermal conditions and mass transfer in this furnace have been studied thoroughly the latest years [7, 8]. This required special care during furnace operation.

Since the resistivity of the final substrates were supposed to be relatively low ($<0.01\,\Omega$ cm), 1.5 g of 95–97% pure boron was added to the charge before melting. Even though – according to phase Si-boron diagrams [9] the melting point of pure boron is about 2100 $^\circ$C, the boron will dissolve completely in the liquid silicon at 1430 $^\circ$C since the solubility is about 10% and the added amount is merely 160 ppm.

The logged data from the casting are shown in Fig. 1.

A complete description of the operation of the furnace under normal conditions has been given earlier [10]. The main differences between standard furnace operation and the one done in this study are:

1. Double layer of coating was used to ensure no sticking between ingot and crucible even with long time at high temperature.
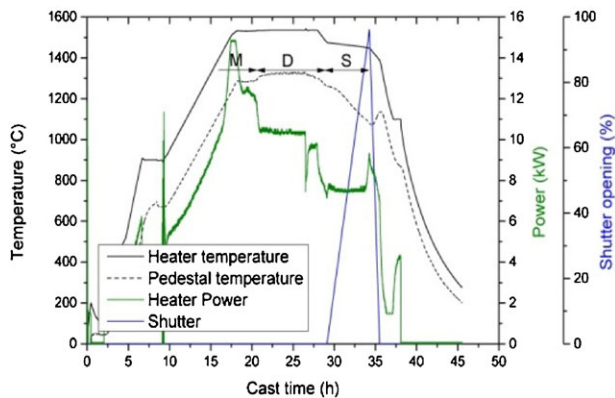
Figure 1 (online color at: www.pss-a.com) Data from the Crystalox furnace during casting. Shown are the heater temperature, pedestal temperature (temperature beneath crucible), heater power, and shutter opening during crystallization. M, D, and S denote melting, dissolution of boron and mixing, and solidification phases, respectively.

2. Since the feedstock was in the form of powder, the initial pump-down phase was done very gentle in order to avoid sucking powder out of the crucible.
3. Gas flow after the vacuum phase was reduced in order not to blow feedstock out of the crucible.
4. After complete melting, the melt was held for 6.5 h longer than normal in order to secure complete dissolution of the boron.

2.2 Wafer samples preparation Highly conductive p+ Si wafers from casted Si ingots were obtained by wire sawing.

Additionally series of Si wafers were produced by thermal spray route, with thicknesses between 300 and 1000 μm, and dimensions $65 \times 50\,mm^2$ have been prepared from nominally un-doped low-cost Si powder. Silicon layers (wafers) were detached from specially selected and prepared substrates/moulds without breaking (Fig. 2). For the mechanical properties measurements sintered wafers were cut on $1 \times 1\,cm^2$ smaller pieces by laser. Summary of samples material and process routes can be seen from Table 1.

Table 1 Summary of samples material and process routes.

sample name	material	process route
Si powder-based multi	Elkem powder	ingot sintering/VGF furnace
P-type multi	solar grade Si	conventional casting
as cut P-type C7	solar grade Si	Czochralski growth
Spray 1	Elkem powder/100% Si	thermal spray
Spray 2	Elkem powder 3% Al/97% Si	thermal spray

3 Measurement of electrical properties Resistivity measurements have been performed by the four-probe method. It has been found that Si wafers fabricated from the casted Si ingot have resistivity <0.01 Ω cm. Such wafers can be used as highly supporting ones for thin Si-based solar cells. Si wafers processed by thermal spray from nominally non-doped low-cost Si powder demonstrated resistivity in the range of 1–10 Ω cm, which shows that sintering process upon thermal spray has been done properly and no barriers between grains have been created. Since this work is focused on mechanical properties of Si powder-based substrates, doping issues for thermal sprayed substrates were not addressed. However, it can be noted that processing of such wafers using highly doped Si powder should result in highly doped and therefore highly conductive substrates.

4 Measurement of mechanical properties

4.1 Experimental set-up In order to assess the mechanical strength of the wafer produced by the new process routes, the ring-on-ring test was used. Based on the recommendations of the ASTM standard C1499-08 [11], a smaller experimental set-up has been designed as illustrated in Fig. 3. This set-up has been selected to measure the material intrinsic strength and avoid the effect of edge defects.

Figure 2 (online color at: www.pss-a.com) Si wafers ($65 \times 50\,mm^2$) fabricated by thermal spray.
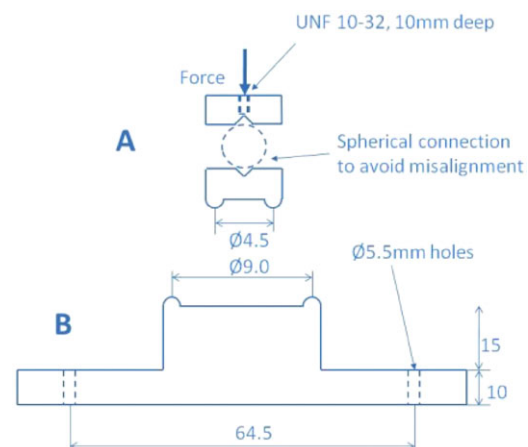
Figure 3 (online color at: www.pss-a.com) Schematic view of the experimental set-up.

4.1.1 Testing equipment The first tests were performed in the Bose Electroforce 250N test machine on lower speeds (i.e., 0.1–0.2 mm min^{-1}). Due to irregular loading rate at the lower speeds, the speed was increased to 1 mm min^{-1}. Nevertheless irregular jumps of the machine remains and it led to machine change for the rest of the study. Therefore only Si powder-based multi samples have been tested using Bose Electroforce 250N machine. An Instron 2kN test machine was used instead in all the remaining experimental work presented in this paper (P-type multi, As cut P-type C7, Spray 1 and Spray 2).
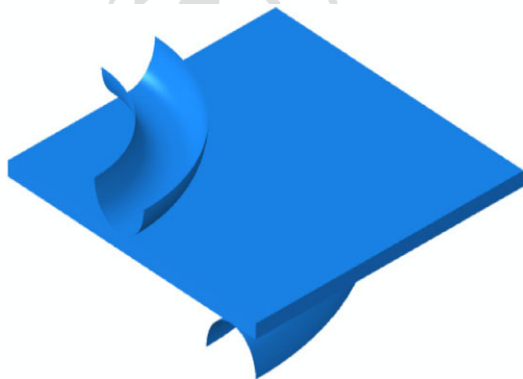
The fixture was made of heat-treated steel, hardened to about 40 HRC.

The data acquisition sampling rate was 100 Hz for the tests done in the Bose machine and 15 Hz for the Instron machine.

4.1.2 Calibration Both test machines were recently calibrated by the manufacturer. Due to limited utilization of the load cell of the Instron machine an additional control was performed with one of the reference load cells of the test laboratory. Check of coaxiality of the test fixture was done during mounting, both by visual inspection and by using premachined pin holes in the center of the upper and lower fixture and a guiding pin. The plane parallelism of the upper and lower ring was corrected before each test by visual inspection of a light gap of about 0.25 mm between the upper and lower ring. The light gap was checked in two perpendicular directions. The fixture was thoroughly cleaned before each test in order to prevent silicon debris deposition on the ring surfaces.

4.2 Numerical model A numerical model of the ring-on-ring mechanical test has been established. The main objectives were to assess the uniformity of the stress distribution inside the loading ring area (especially at the contact point) and develop a formula to compute directly the maximal principal stress for the displacement and the sample thickness.

The model was developed using Abaqus/Standard 6.11 with implicit time integration. Only a quarter of the sample and rings is modeled (see Fig. 4). The sample mesh size is

0.05 mm. The material properties are indicated in Table 2. The dimensions and element type are provided in Table 3.

As illustrated in Fig. 5, considering the thinnest sample which is the most critical in terms of stress distribution, the stress inside the loading ring is quite homogeneous and a relatively small increase (∼5%) is observed only in the contact area with the loading ring. Therefore the dimensions of the sample and the rings are adequate for wafer strength measurements.

By applying the model to various thicknesses (0.20, 0.39, 0.6, and 0.8 mm) and performing a regression analysis, we obtained the following formula:

$$\sigma = (2616h + 3067)\delta^2 + (14\,830h - 465)\delta, \tag{1}$$

**Table 2** Silicon properties for the numerical model.

material	silicon
model	isotropic elasticity
Young's modulus	162.5 GPa
Poisson's ratio	0.223

Table 3 Numerical model dimensions and element type.

part	shape	finite element model
silicon specimen	square^a (10 × 10)	8-nodes brick element
loading ring	ring^b (4.5 × 0.5)	shell, discrete rigid
support ring	ring^b (9 × 0.5)	shell, discrete rigid

^{a}Length and width in mm.
^{b}Diameter and curvature radius in mm.

Figure 4 (online color at: www.pss-a.com) Abaqus model of the ring-on-ring test.
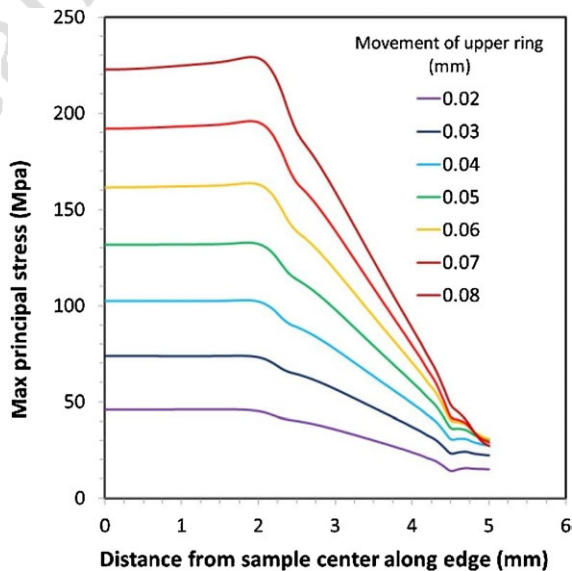

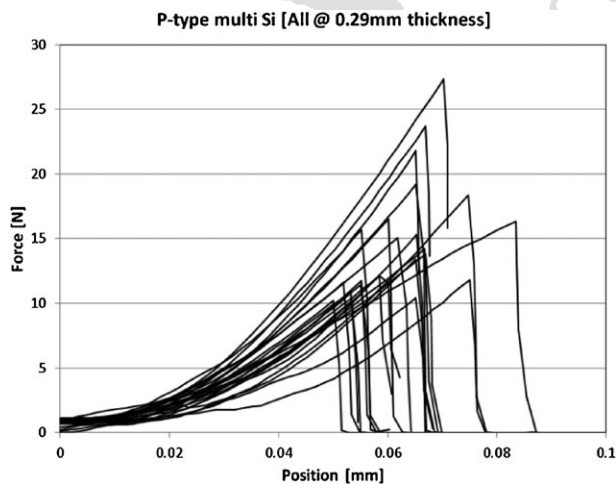**Figure 5** (online color at: www.pss-a.com) Stress distribution along the cross-section of the sample (thickness: 0.2 mm).

where σ is the stress at the sample center in MPa, h is sample thickness in mm, and δ is the displacement in mm.
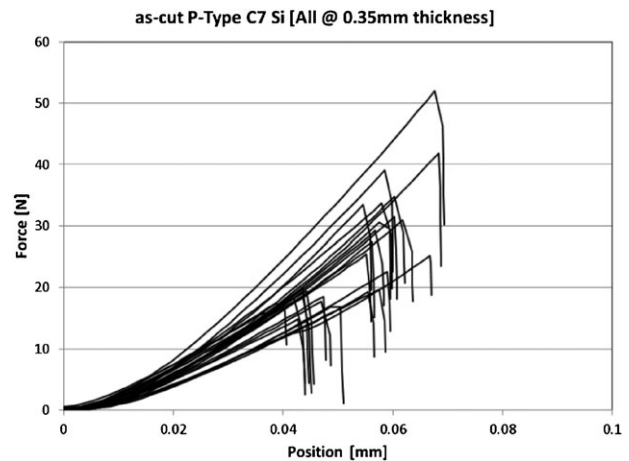
5 Results and analysis The raw data from the series of mechanical tests using the ring-on-ring set-up previously described are presented in Figs. 6–10. The displacement of the ring is given in the x-axis while the y-axis provides the applied force measured by the load cell. As mentioned in the Section 4.1, the curves of the initial set-up (Fig. 6) using the Bose Electroforce 250N test machine has a stair case appearance. Nevertheless it does affect neither the curve shape nor the displacement at fracture. The main issue in this series of test is the large variation in the slope of the curves before the peak force value is reached. We would expect for such material (except maybe for the spray samples) a very reproducible elastic response. Indeed we have previously measured the strength of the Si powder based multi samples

Figure 8 Force displacement curves for the As cut P-type C7 samples (25 samples).
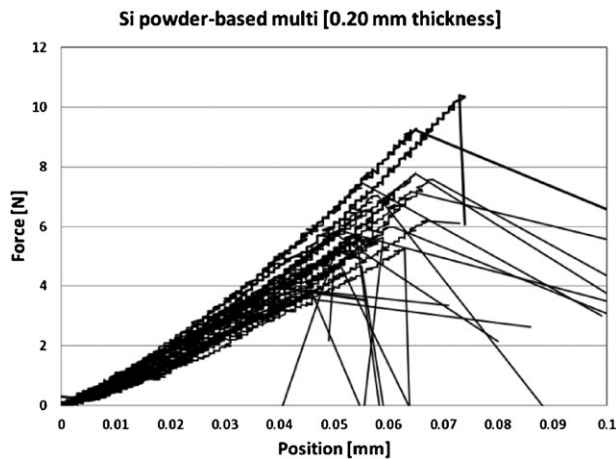
Figure 6 Force displacement curves for the Si powder-based multi samples (28 samples).

using the 4pt-bending test and the curves were overlapping. The reason for this discrepancy is not clearly identified but there are two possible explanations. First, as mentioned by Cotterell et al. [12], the proper positioning of the samples for the ring-on-ring test could be an issue. Friction between the ring and the sample can lead to inaccurate results. Therefore, Wasmer et al. [13] recommend the use of carbon paper. Please note that the Weibull fit of the experimental data without carbon paper from Wasmer et al. shows a similar staircase aspect as some of our results (especially Fig. 12 where one can observe a slope change for the experimental curves between a probability of 0.4 and 0.5). It is also important to note that this friction effect might be dependent on sample roughness which varies between our materials. Nevertheless we assume that these effects induce only a systematic error on the force measurements. Therefore the analysis of the results based on the displacement should
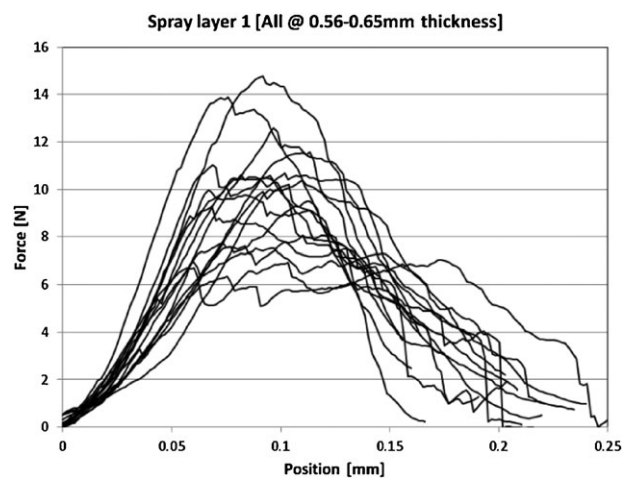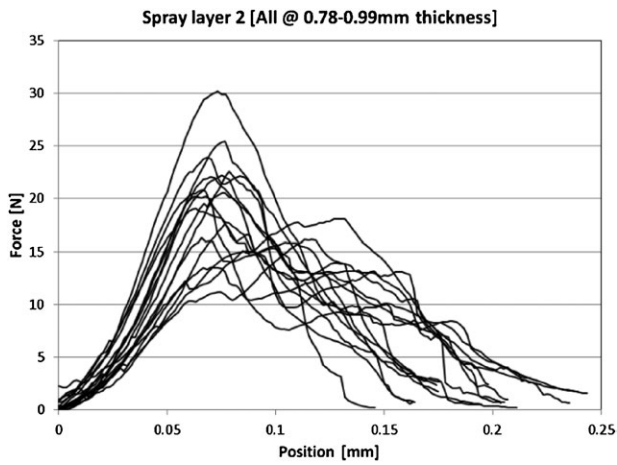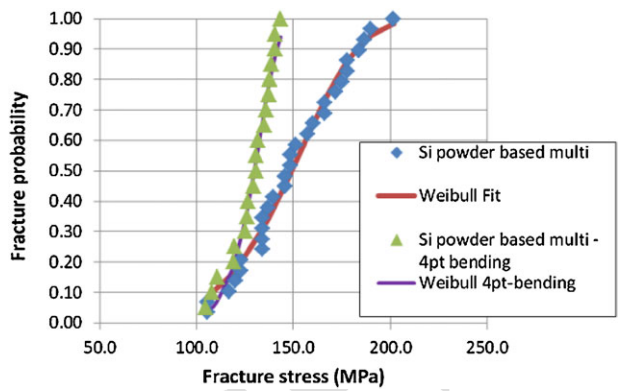

Figure 7 Force displacement curves for the P-type multi samples (23 samples).

Figure 9 Force displacement curves for the Spray 1 samples (16 samples).

Figure 10 Force displacement curves for the Spray 2 samples (16 samples).

Figure 11 (online color at: www.pss-a.com) Strength measurements and Weibull fit for Si powder based multi samples using ring-on-ring test ($\sigma_0 = 158$ MPa and $m = 5.9$) compared with 4pt-bending experimental measurements ($\sigma_0 = 133$ MPa and $m = 14$).

provide good estimate of the samples strength for comparison between different materials.

The raw data has been post-processed using Eq. (1). Then the stress values at fracture were ordered and related to a probability in order to build the Weibull distribution.

Indeed the standard parameters in the literature to assess the wafer strength are the parameters based on the Weibull distribution.

The probability of fracture is described by an exponential function with two parameters:

$$P(\sigma) = 1 - e^{-(\sigma/\sigma_0)^m}. \tag{2}$$

From the ordered values, a curve fitting procedure has been applied in Excel. The results for the three first materials are presented in Figs. 11–13. In addition, previous results with Si powder based multi samples obtained with 4pt-bending set-up and larger samples (5×5 mm^2) are also presented for comparison.

As illustrated by Figs. 9 and 10, the material behavior of the spray samples is significantly different. Therefore the direct application of the previous procedure is not possible and the study of the sprayed samples requires a more detailed analysis of the material. In all the previous cases we assume that the material properties are similar to bulk silicon which is a quite good approximation. Nevertheless for the sprayed samples, the microstructure of the material is non-homogeneous which is mainly due to the presence of porosity and layers.

In order to obtain a better estimate of the equivalent fracture stress for this material, we will need to first estimate the porosity and subsequently estimate the relative correction of the stress value resulting from this porosity. As illustrated on Fig. 14, the metallography image for Si sample Spray 1 is processed using a simple threshold method in order to detect the holes and estimate the porosity.

This procedure is not the most advanced and provides only an estimate of the porosity. Using this technique we obtain a
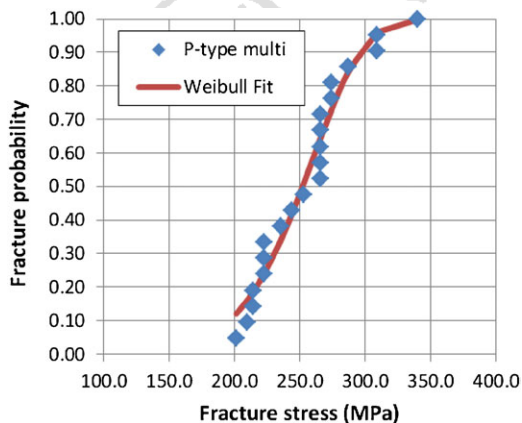
Figure 12 (online color at: www.pss-a.com) Strength measurements and Weibull fit for P-type multi samples ($\sigma_0 = 264$ MPa and $m = 7.5$).
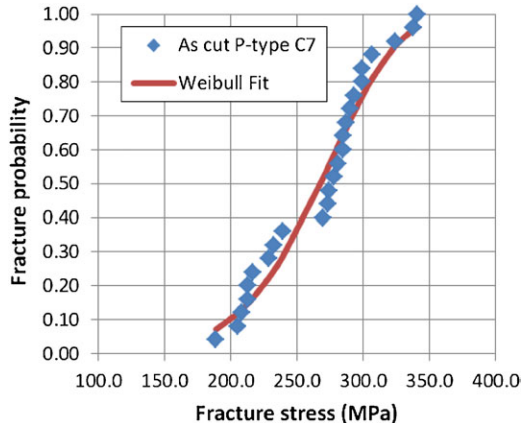
Figure 13 (online color at: www.pss-a.com) Strength measurements and Weibull fit for P-type multi samples ($\sigma_0 = 283$ MPa and $m = 6.4$).
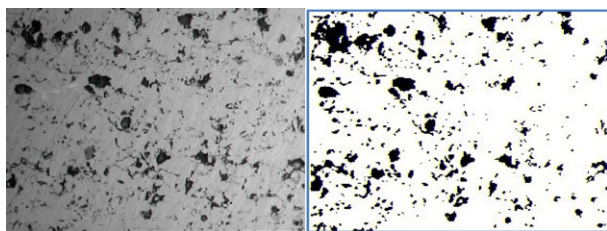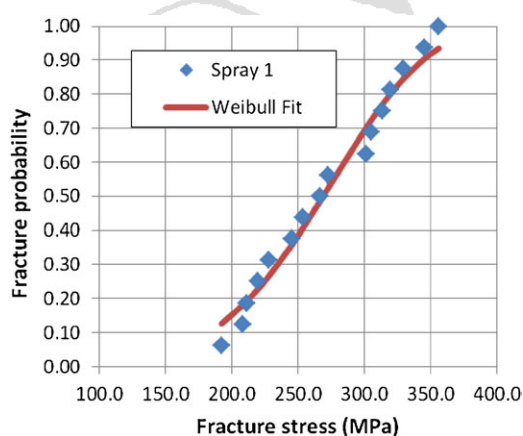
Figure 14 Comparison between initial metallography image (×500) on the left and processed image for porosity estimate on the right.

Figure 16 (online color at: www.pss-a.com) Strength measurements and Weibull fit for P-type multi samples ($\sigma_0 = 303$ MPa and $m = 9$).
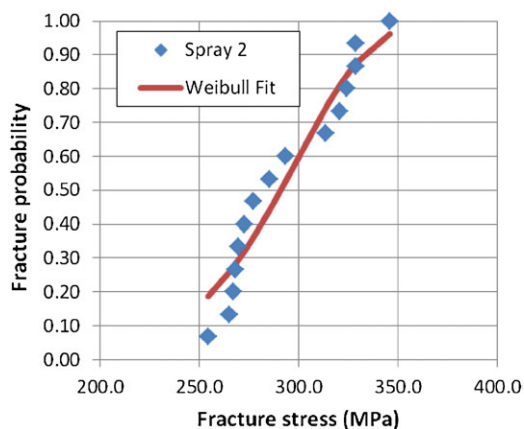
1 value of 11% porosity, which agrees with the results obtained
2 for other type of powder based materials (yttria-stabilized
3 zirconia coatings) processed by thermal spray [14].
4   In the work by Wang et al. [14], different spraying
5 techniques are used with increasing level of porosity and the
6 effect on the elasticity modulus for each sample is measured.
7 Two values are closed to our porosity estimate: 7.6% and
8 12.2% porosity for which the elasticity modulus is reduced to
9 45% and 25% of the bulk value, respectively. From these
10 values, we obtain by simple interpolation a decrease to 30%
11 of the elasticity modulus of bulk silicon. Various materials
12 sprayed using high velocity oxygen fuel technique (HVOF)
13 ranged also between 30% and 40% of the bulk elastic
14 modulus [15].
15   Therefore, in order to estimate the fracture stress using
16 the previous formula, we apply a corrective multiplicative
17 factor of 0.3 to the fracture stress computed from the
18 displacement at rupture (Eq. 1). The results are presented in
19 Figs. 15 and 16. Please note that these values are sensitive to
20 the sample thickness (not precisely measured over the whole
21 surface of the sample and to the porosity (estimated for only
22 one sample) and therefore this analysis will provide only
23 a coarse estimate of the material strength. In any case, as
24 presented by Margadant et al. [16], it is very difficult to
25 obtain an accurate value of the elastic modulus of a coating as
26 it depends on the measurement and spraying technique used.

Table 4 Summary of the Weibull fit of the ring-on-ring tests (or 4pt-bending when specified).

material	Weibull mean stress, σ_0	Weibull variance, m
Si powder based multi	158	5.9
Si powder based multi (4pt bending)	133	14
P-type multi	264	7.5
as cut P-type C7	283	6.4
Spray 1	290	4.8
Spray 2	303	9

1   For comparison the results for the five materials are
2 summarized in Table 4. As expected the variance for all
3 materials is in the same range except for the 4pt-bending test
4 where usually a larger variance is obtained.
5   It is also worth mentioning the significant increase
6 between Spray 1 and Spray 2 samples. This might be
7 explained by an influence of 3% of Al powder, which is
8 mixed with Si powder based feedstock on mechanical
9 properties of sprayed Si wafers. More detailed studies are
10 required to investigate this effect.

11   **6 Conclusions** Comparative analysis of mechanical
12 properties of Si samples obtained from new process routes
13 for the production of silicon wafers has been presented.
14 Characterization of the mechanical strength of the different
15 silicon samples was investigated using a ring-on-ring test.
16 The maximum principal stresses at failure during bending
17 were calculated to indicate the fracture strength and fitted to a
18 Weibull distribution. The study showed that:
20

Figure 15 (online color at: www.pss-a.com) Strength measurements and Weibull fit for P-type multi samples ($\sigma_0 = 290$ MPa and $m = 4.8$).

21 • In spite of some experimental challenges, the ring-on-ring
   set-up provided acceptable estimate of the material for
22 various materials and process routes.

- The Si powder based multi samples were the weaker but still with a reasonable strength comparable to standard wafer without etching.
- The spray samples display a specific material behavior due to porosity and layering. Nevertheless the final material strength is high.

As a summary, this work has demonstrated the potential of new process routes leading to the production of Si wafers with adequate material properties both electrical and mechanical.

It can be concluded that Si powder-to-substrate approach can be utilized for the processing of Si based supporting substrates, which potentially are fully compatible with the deposition/crystallization processes of thin Si layers on top of such substrates and posses comparable with multi-Si/Cz-Si substrates mechanical properties.

Further work should be performed to analyze in more details the microstructure of the new materials and assess their downstream integration in the solar cell production.

References

[1] R. Brendel and D. Scholten, Appl. Phys. A **69**, 201 (1999).

[2] www.eupvplatform.org.

[3] A. V. Shah, J. Meier, E. Vallat-Sauvain, N. Wyrsh, U. Kroll, C. Droz, and U. Graf, Sol. Energy Mater. Sol. Cells **78**, 469 (2003).

[4] A. M. Barnett, J. A. Rand, R. B. Hall, J. C. Bisaillon, E. J. DelleDonne, B. W. Feyock, D. H. Ford, A. E. Ingram, M. G. Mauk, J. P. Yaskoff, and P. E. Sims, Sol. Energy Mater. Sol. Cells **66**, 45 (2001).

[5] E. Schmich, N. Schillinger, and S. Reber, Surf. Coat. Technol. **201**, 9325 (2007).

[6] S. Janz, S. Reber, F. Lutz, and C. Schetter, Thin Solid Films **511–512**, 271 (2006).

[7] E. A. Meese et al., 20th European Photovoltaic Solar Energy Conference, Barcelona, Spain[Q2] (2005), pp. 909–913.

[8] H. Laux et al., 20th European Photovoltaic Solar Energy Conference, Barcelona, Spain (2005), pp. 1090–1094.

[9] ASM Binary Phase Diagrams,[Q3] second ed. (ASM International, Materials Park, Ohio, USA, 1996).

[10] Ø. Mjøs, Ph. D. thesis, 109 NTNU, Trondheim Norway (2006), p. 112.[Q4]

[11] Standard Test Method for Monotonic Equibiaxial Flexural Strength of Advanced Ceramics at Ambient Temperature, ASTM C1499-08.

[12] B. Cotterell et al., Trans. ASME[Q5] **125** (2003).

[13] K. Wasmer et al., 22nd European Photovoltaic Solar Energy Conference, Milan, Italy (2007).

[14] Z. Wang et al., Acta Mater. **51**, 5319 (2003).

[15] J. Pina, A. Dias, J. L. Lebrun et al., Mater. Sci. Eng. A **267**, 130 (1999).

[16] N. Margadant et al., Surf. Coat. Technol. **200**, 28050 (2006).

Q1: Author: Please expand the forename of the authors R. Gløckner, M. Syvertsen and also check the telephone number of the corresponding author.

Q2: Author: As per the style of the journal, et al. is not allowed in the reference list. Please check all the et al. references.

Q3: Author: Please provide the author names.

Q4: Author: Please check the presentation of this reference.

Q5: Author: Please provide the page range.

## USING e-ANNOTATION TOOLS FOR ELECTRONIC PROOF CORRECTION

Required software to e-Annotate PDFs: <u>Adobe Acrobat Professional</u> or <u>Adobe Reader</u> (version 8.0 or above). (Note that this document uses screenshots from <u>Adobe Reader X</u>)
The latest version of Acrobat Reader can be downloaded for free at: <u>http://get.adobe.com/reader/</u>

Once you have Acrobat Reader open on your computer, click on the Comment tab at the right of the toolbar:

🗋 🖫 🖶 ✉ | ⬆ ⬇ | 1 / 27 | ⊖ ⊕ | 70.4% ▾ | 🖫 | ↔ ▾ | **Tools** **Comment** **Share**
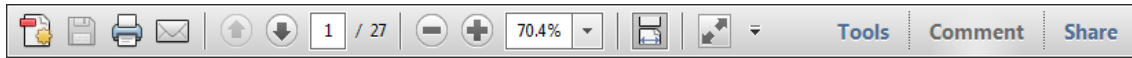
This will open up a panel down the right side of the document. The majority of tools you will use for annotating your proof will be in the Annotations section, pictured opposite. We've picked out some of these tools below:
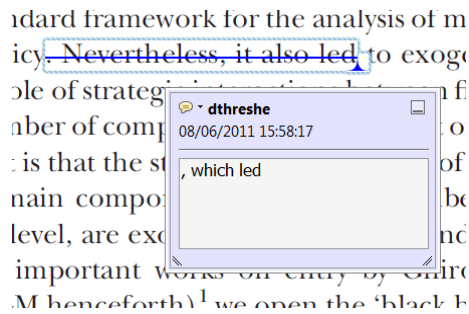
▾ **Annotations**

---
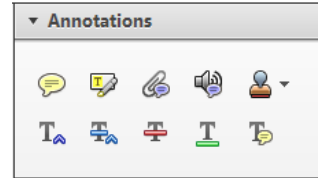
1. **Replace (Ins)** Tool – for replacing text.

Strikes a line through text and opens up a text box where replacement text can be entered.

How to use it
- Highlight a word or sentence.
- Click on the Replace (Ins) icon in the Annotations section.
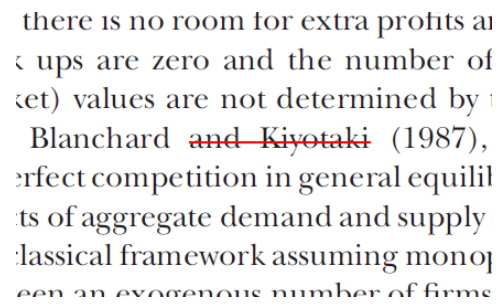- Type the replacement text into the blue box that appears.

dard framework for the analysis of m
icy. Nevertheless, it also led to exoge
ble of strategic interaction between fi
mber of comp...   o
: is that the st...   of
nain compo...   bo
level, are exc...   nd
important works on entry by ...
M henceforth)[1] we open the 'black b

dthreshe
08/06/2011 15:58:17
, which led

---

2. **Strikethrough (Del)** Tool – for deleting text.

Strikes a red line through text that is to be deleted.

How to use it
- Highlight a word or sentence.
- Click on the Strikethrough (Del) icon in the Annotations section.

there is no room for extra profits a
: ups are zero and the number of
:et) values are not determined by
. Blanchard and Kiyotaki (1987),
erfect competition in general equili
ts of aggregate demand and supply
:lassical framework assuming mono
:een an exogenous number of firms

---

3. **Add note to text** Tool – for highlighting a section to be changed to bold or italic.
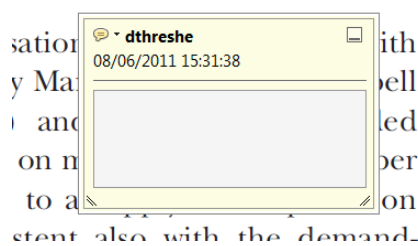
Highlights text in yellow and opens up a text box where comments can be entered.

How to use it
- Highlight the relevant section of text.
- Click on the Add note to text icon in the Annotations section.
- Type instruction on what should be changed regarding the text into the yellow box that appears.

namic responses of mark ups
ent with the VAR evidence

sation...   ith
y Ma...   ell
 and...   led
on n...   ber
to a...   on
:tent also with the demand-

dthreshe
08/06/2011 15:31:38

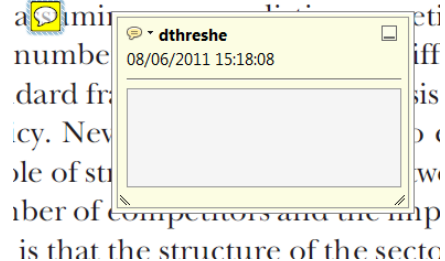### 4. **Add sticky note** Tool – for making notes at specific points in the text.

Marks a point in the proof where a comment needs to be highlighted.

How to use it
- Click on the Add sticky note icon in the Annotations section.
- Click at the point in the proof where the comment should be inserted.
- Type the comment into the yellow box that appears.

land and supply shocks. Most or
a... min... ... eti
numbe... ... iff
dard fra... sis
icy. Nev... e
ble of st... w
ber of competitors and the imp
is that the structure of the secto

dthreshe
08/06/2011 15:18:08

USING e-ANNOTATION TOOLS FOR ELECTRONIC PROOF CORRECTION

5. Attach File Tool – for inserting large amounts of text or replacement figures.

Inserts an icon linking to the attached file in the appropriate pace in the text.

How to use it

- Click on the Attach File icon in the Annotations section.
- Click on the proof to where you'd like the attached file to be linked.
- Select the file to be attached from your computer or network.
- Select the colour and type of icon that will appear in the proof. Click OK.

END

0.20

0.15

0.10

0.05
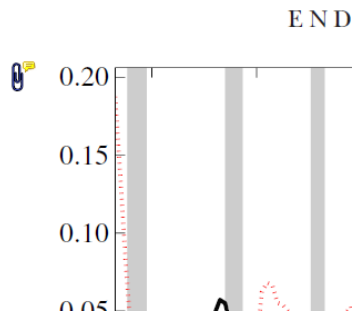
## 6. Add stamp Tool – for approving a proof if no corrections are required.

Inserts a selected stamp onto an appropriate place in the proof.

How to use it

- Click on the Add stamp icon in the Annotations section.
- Select the stamp you want to use. (The Approved stamp is usually available directly in the menu that appears).
- Click on the proof where you'd like the stamp to appear. (Where a proof is to be approved as it is, this would normally be on the first page).

or the business cycle, starting with the . on perfect competition, constant ret production. In this environment goods extra profits and the structure of market he n ... APPROVED ... p etermined by the model. The New-Key otaki (1987), has introduced produc general equilibrium models with nomin nd and supply shocks. Most of this literat
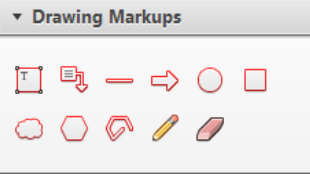
7. Drawing Markups Tools – for drawing shapes, lines and freeform annotations on proofs and commenting on these marks.
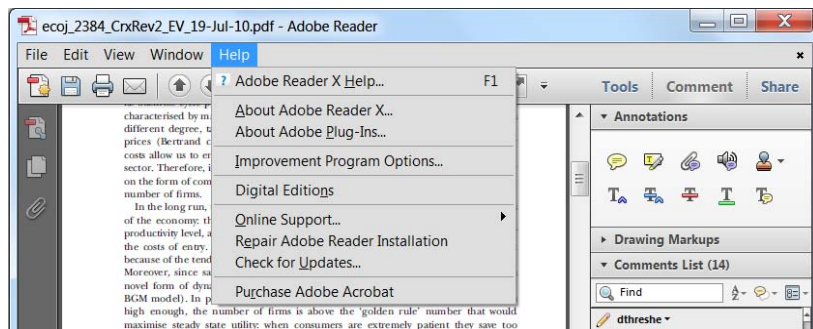
Allows shapes, lines and freeform annotations to be drawn on proofs and for comment to be made on these marks..

How to use it

- Click on one of the shapes in the Drawing Markups section.
- Click on the proof at the relevant point and draw the selected shape with the cursor.
- To add a comment to the drawn shape, move the cursor over the shape until an arrowhead appears.
- Double click on the shape and type any text in the red box that appears.

dthreshe
08/06/2011 16:23:54

Move to the bottom of the left column of panels.
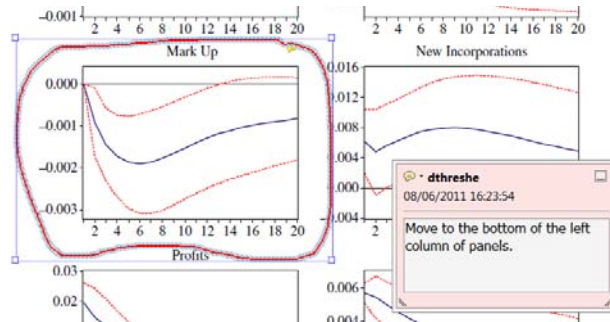
For further information on how to annotate proofs, click on the Help menu to reveal a list of further options:

ecoj_2384_CrxRev2_EV_19-Jul-10.pdf - Adobe Reader

File   Edit   View   Window   Help

? Adobe Reader X Help...   F1

About Adobe Reader X...
About Adobe Plug-Ins...

Improvement Program Options...

Digital Editions

Online Support...
Repair Adobe Reader Installation
Check for Updates...

Purchase Adobe Acrobat

Tools   Comment   Share

▼ Annotations

▶ Drawing Markups

▼ Comments List (14)

Find

dthreshe

Instructions for Proof Corrections and Orders

Please correct your proofs and return them within 4 days together with the completed reprint order form. The editors reserve the right to publish your article with editors' corrections if your proofs do not arrive in time.

After having received your corrections, your paper will be published online soon in the Wiley Online Library (wileyonlinelibrary. com).

Please keep in mind that reading proofs is your responsibility. Corrections should therefore be clear. We prefer the corrections be made directly within the PDF file (see E-annotations instructions). Alternatively, you may provide us with a list of corrections by e-mail, with the corrections referring to their line number.

Manuscript files are sometimes slightly modified by the production department to follow general presentation rules of the journal.

Note that the quality of the halftone figures is not as high as the final version that will appear in the issue.

Check the enclosed proofs very carefully, paying particular attention to the formulas (including line breakings introduced in production), figures, numerical values, tabulated data and layout of the pages.

A black box (■) or a question at the end of the paper (after the references) signals unclear or missing information that specifically requires **your attention.** Note that the author is liable for damages arising from incorrect statements, including misprints.

The main aim of proofreading is to correct errors that may have occurred during the production process, **and not to modify the content of the paper**. Corrections that may lead to a change in the page layout should be avoided.

Note that sending back a corrected **manuscript** file **is of no use**.

Return the corrected proofs within 4 days by e-mail.

Please do not send your corrections to the typesetter but to the Editorial Office:

E-MAIL: pssa.proofs@wiley-vch.de

Please limit corrections to errors in the text; cost incurred for any further changes or additions will be charged to the author, unless such changes have been agreed upon by the editor.

If your paper contains **color figures**, please fill in the Color Print Authorization and note the further information given on the following pages.

Full color reprints, Customized PDF files, Printed Issues, Color Print, and Cover Posters may be ordered by filling in the accompanying form.

Order Form

physica status solidi
www.pss-a.com
applications and materials science

2013

WILEY-VCH GmbH & Co. KGaA
physica status solidi
Rotherstrasse 21
10245 Berlin
Germany

TEL +49 (0) 30–47 03 13 31
FAX +49 (0) 30–47 03 13 34
E-MAIL pssa.proofs@wiley-vch.de

WILEY
Publishers Since 1807

Please complete this form and return it by e-mail or FAX.

Article No.

Author/Title

e-mail address

Required Fields may be filled in using Adobe Reader

Color Print Authorization

Please bill me for

color print figures (total number of color figures)

☐ YES, please print Figs. No. [   ] in color.

☐ NO, please print all color figures in black/white.

Reprints/Issues/PDF Files/Posters

Whole issues, reprints and PDF files (300 dpi) for an unlimited number of printouts are available at the rates given on the next page. Reprints and PDF files can be ordered before *and after* **publication of an article. All reprints will be delivered in full color, regardless of black/white printing in the journal.**

Reprints

Please send me and bill me for

full color reprints with color cover

full color reprints with personalized color cover

Issues

Please send me and bill me for

entire issues

Customized PDF-Reprint

Please send me and bill me for

☐ a PDF file (300 dpi) for an unlimited number of printouts **with customized color cover sheet.**

The PDF file will be sent to your e-mail address.

Send PDF file to:

Please note that posting of the final published version on the open internet is not permitted. For author rights and re-use options, see the Copyright Transfer Agreement at http://www.wiley.com/go/ctavchglobal.

Cover Posters

Posters are available of all the published covers in two sizes (see attached price list). **Please send me and bill me for**

A2 (42 × 60 cm/17 × 24in) posters

A1 (60 × 84 cm/24 × 33in) posters

Mail reprints and/or issues and/or posters to (no P.O. Boxes):

VAT number:

Information regarding VAT

Please note that from German sales tax point of view, the charge for **Reprints, Issues or Posters** is considered as **"supply of goods"** and therefore, in general, such delivery is a subject to German sales tax. However, this regulation has no impact on customers located outside of the European Union. Deliveries to customers outside the Community are automatically tax-exempt. Deliveries within the Community to institutional customers outside of Germany are exempted from the German tax (VAT) only if the customer provides the supplier with his/her VAT number.

The VAT number (value added tax identification number) is a tax registration number used in the countries of the European Union to identify corporate entities doing business there. It starts with a country code (e.g. FR for France, GB for Great Britain) and follows by numbers.

The charge for **front cover/back cover/inside cover pictures, color figures or frontispieces publications** is considered as **"supply of services"** and therefore it is a subject to German sales tax. However, in case you are an institutional customer outside of Germany, the tax can be waived if you provide us with the VAT number of your company.

Customers outside of the EU may have a VAT number starting with "EU" instead of the country code if they are registered by the EU's tax authorities. In case you do not have a VAT number of EU and you are a taxable person doing business in a country outside EU, then please provide us with a certification from your local tax authorities confirming that you are a taxable person under the local tax law. Please note that the certification needs to confirm that you are a taxable person and you are conducting an economic activity in your country. Certifications which confirm that you are tax-exempt legal body (non-profit organization, public body, school, political party, etc.) in your country cannot be accepted for the German VAT purposes.

Purchase Order No.:

Terms of payment:

☐ Please send an invoice   ☐ Cheque is enclosed

☐ **VISA, MasterCard and AMERICAN EXPRESS.**

Please use this link (Credit Card Token Generator) to create a secure Credit Card Token and include this number in the form instead of the credit card data.

https://www.wiley-vch.de/editorial_production/index.php

CREDIT CARD TOKEN NUMBER:

Send invoice to:

Signature _____

Date _____

Please use this form to confirm that you are prepared to pay your contribution.

Please sign and return this page.

You will receive an invoice following the publication of your article in the journal issue.

Price List – pss (a) 2013

Reprints/Issues/PDF-Files/Posters

WILEY *Publishers Since 1807*

The prices listed below are valid only for orders received in the course of 2013. Minimum order for reprints is 50 copies. **Reprints can be ordered before *and after* publication of an article. All reprints are delivered with color cover and color figures**. If more than 500 copies are ordered, special prices are available upon request.

Single issues are available to authors at a reduced price.

The prices include mailing and handling charges. All prices are subject to local VAT/sales tax.

Reprints with color cover	Price for orders of (in Euro)					
Size (pages)	50 copies	100 copies	150 copies	200 copies	300 copies	500 copies*
1– 4	345	395	425	445	548	752
5– 8	490	573	608	636	784	1077
9–12	640	739	786	824	1016	1396
13–16	780	900	958	1004	1237	1701
17–20	930	1070	1138	1196	1489	2022
for every additional 4 pages	147	169	175	188	231	315
for personalized color cover	**190**	**340**	**440**	**650**	**840**	**990**

PDF file (300 dpi, unlimited number of printouts, customized cover sheet) € 330

Issues € 48 per copy for up to 10 copies.*

Cover Posters
- A2 (42 × 60 cm/17 × 24in) € 49
- A1 (60 × 84 cm/24 × 33in) € 69

*Prices for more copies available on request.

> **Special offer: If you order 100 or more reprints you will receive a pdf file (300 dpi, unlimited number of printouts, color figures) and an issue for free.**

Color figures

If your paper contains **color figures**, please notice that, generally, these figures will appear in color in the online PDF version and all reprints of your article at no cost. This will be indicated by a note "(online color at: www.pss-a.com)" in the caption. The print version of the figures in the journal hardcopy will be black/white unless the author explicitly requests a color print publication and contributes to the additional printing costs.

	Approximate color print figure charges
First figure	€ 495
Each additional figure	€ 395 Special prices for more color print figures on request

If you wish color figures in print, please answer the **color print authorization** questions on the order form.